Supplementary Information

Highly efficient field-free switching by orbital Hall torque in a MoS_2-based device operating at room temperature

Antonio Bianco [1,2,**], Michele Ceccardi [1,**], Raimondo Cecchini [3], Daniele Marré [1,2], Chanchal K. Barman [4], Fabio Bernardini [4], Alessio Filippetti [4,5], Federico Caglieris [2], Ilaria Pallecchi [2,*]

[1] *Department of Physics, University of Genova, Via Dodecaneso 33, 16146 Genova, Italy*
[2] *CNR-SPIN, Institute for superconductors, innovative materials and devices, Corso Perrone 24, 16152 Genova, Italy*
[3] *CNR-ISMN, Institute for the study of nanostructured materials, via Gobetti 101, 40129 Bologna, Italy*
[4] *Dipartimento di Fisica, Università di Cagliari, Cittadella Universitaria, Monserrato (Ca) 09042, Italy*
[5] *CNR - Istituto Officina dei Materiali (IOM) Cagliari, Cittadella Universitaria, Monserrato (CA), 09042, Italy*
[**] *These two authors contributed equally to the work*
[*] *Corresponding author: Ilaria.pallecchi@spin.cnr.it*

1. H cycles at different AC above-threshold currents and frequencies

Fig.s S1 and S2 show the differential voltage between the Co electrodes, measured while cycle-sweeping the applied field parallel to the direction that connects the electrodes and applying a current to the underneath MoS_2. Different values of above-threshold current (Fig. S1) and different frequencies (Fig. S2) are displayed. In Fig. S1, the magnitude of the voltage steps exhibits no clear dependence on the magnitude of the current, as long as the latter exceeds the threshold $|I_{peak}|>1.6$ mA. Only at the largest current 6 mA the step is slightly smaller, possibly due to slight Joule heating and consequent thermally assisted magnetic switching. This effect is however minor, thanks to the large Curie temperature of Co.
In Fig. S2, it is shown that measurement frequency plays no significant role either.

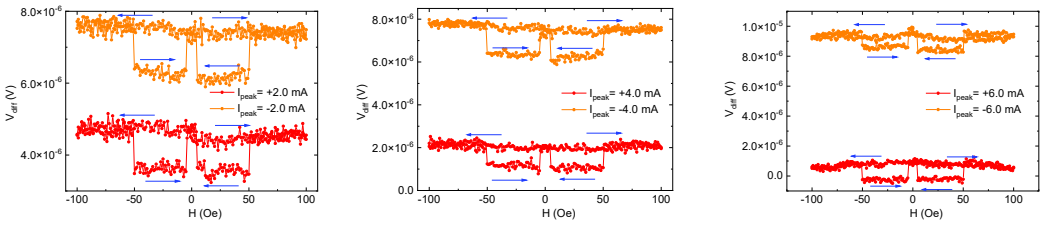

Fig. S1. H cycles of differential voltage between the Co electrodes, for applied charge currents in MoS_2 $I=I_0+\Delta I \sin(\omega t)$, with positive and negative above-threshold values of $I_{peak}=2xI_0$ and $\Delta I=|I_0|$.

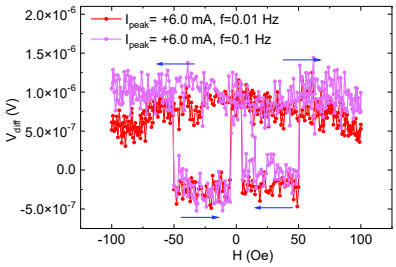

Fig. S2. H cycle of differential voltage between the Co electrodes, for applied charge currents in MoS_2 $I=I_0+\Delta I \sin(\omega t)$, with I_{peak}=+6.0mA and frequencies f=0.01 and 0.1 Hz.

2. Current sweeps performed with different protocols

Fig.S3 shows different measurements of differential voltage between the Co electrodes at fixed H, varying the applied sinusoidal current $I=I_0+\Delta I \sin(\omega t)$, always with $\Delta I=|I_0|$. The current I_0 was either swept cyclically back and forth (panels S3a and S3b) or swept one-way from zero to a maximum value, either positive or negative, in such a way that no current inversion occurs in each run at fixed field (panels S3c and S3d).

In Fig. S3a, measurements with current cycles are displayed. Note that in this case, not the same hysteresis as in H cycles is expected, due to the different protocol of reversing the sign of the current at each fixed field. It is evident that there is an offset of some curves with respect to others, indicating that an additional non-ohmic voltage is present in some curves. In Fig. S3b, the intercepts of linear fits to data in Fig. S3a are shown. A clear two-level behavior is observed, evidencing this additional non-ohmic voltage. Furthermore, plotting the voltage for the four different branches of the current cycles (inset of Fig. S3b), we observe a similar pattern for H=+100 Oe and H=-100 Oe, and another similar pattern for H=+30 Oe and H=-30 Oe.

In Fig. S3c, the current is swept with I_{peak} from 1 to 6 mA at different fixed field values (+100 Oe, +25 Oe, 0, -100 Oe, -25 Oe and 0, in this sequence), and successively from 1 to -6 mA at the same fixed field values. In this measurement protocol, the current sign is not reversed at fixed field. In this plot, there is the same clear offset of some curves with respect to others, as observed in Fig. S3a. This is better seen in Fig. S3d, where the intercepts of the linear fits are plotted. Two features are clearly observed: a two level behavior and a hysteresis as a function of H, whose clockwise/anticlockwise direction is determined by the sign of the current.

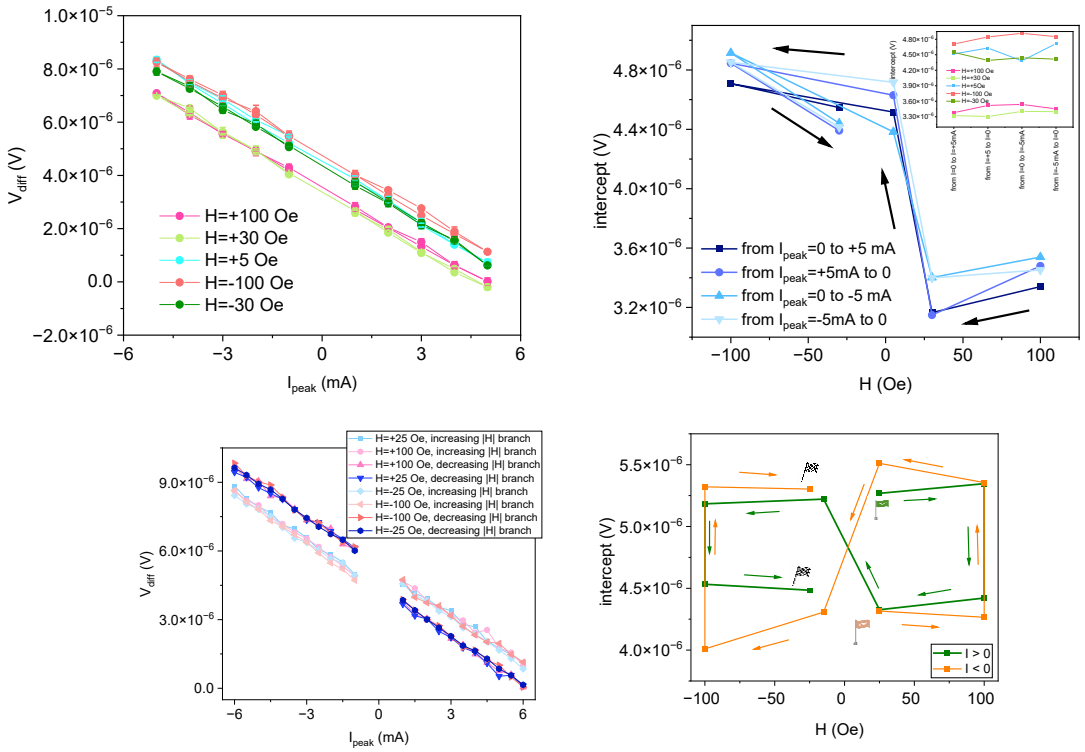

Figure S3: a) Differential voltage between Co electrodes, measured in cycles of applied current $I=I_0+\Delta I \sin(\omega t)$, with I_{peak} ($\Delta I=|I_0|$, $I_{peak}=2xI_0$) varied as +1 mA → +5 mA → -1 mA → -5 mA → 0 at fixed H values +100 Oe, +30 Oe, +5 Oe, -100 Oe and -30 Oe, applied in this order. The straight lines are linear fits of data. b) The intercepts of the linear fits of data in panel a) are plotted as a function of the applied field. The arrows indicate the chronological order of current sweeps and the inset shows the same intercept values plotted as a function of the successive branches of the current sweeps.

c) Differential voltage between Co electrodes, measured in sweeps of applied current $I=I_0+\Delta I \sin(\omega t)$, with positive current I_{peak} ($\Delta I=|I_0|$, $I_{peak}=2xI_0$) increasing from +0.5 mA to +6 mA in steps of 0.5 mA, carried out at different fixed field values (100 Oe, 25 Oe, 0, -100 Oe, -25 Oe and 0, in this sequence) and then with negative current I_{peak} ($\Delta I=|I_0|$,$I_{peak}=2xI_0$) varying from -0.5 mA to -6 mA in steps of -0.5 mA, at the same field values. d) Intercepts of the linear fit of panel c) are plotted as a function of the applied field. The

arrows indicate the chronological order of current sweeps and the flags indicate the starting and ending points of the measurements for positive and negative current.

3. Magnetotransport characterization of the MoS_2 flake

Transport properties of the MoS_2 flake were characterized. The room temperature resistivity, carrier density and mobility are 3.5×10^{-4} Ωm, ~10^{18} cm^{-3} and ~150 $cm^2/(Vs)$, respectively. The resistivity has a semiconducting temperature behaviour with thermal activation energy ~80 meV.

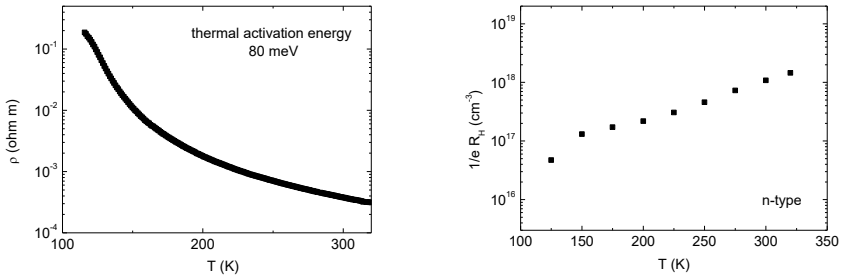

Fig. S4. Left panel: temperature dependence of MoS_2 resistivity, exhibiting semiconducting behaviour. Right panel: carrier concentration measured by Hall effect.

4. Calculation of SHE and OHE in bulk MoS_2

In this work we were primary interested in the spin and orbital currents flowing along the z-direction (c-axis) and polarized in-plane (y-direction) induced by an electric field with an in-plane direction (x-direction). For completeness and with the same procedure we computed also the other components of the Hall conductivity tensor. Overall, there are 27 components of this tensor. Excluding components having field/current parallel to polarization direction or current parallel to field, there remains 6 components. Exchanging the field with the current direction will change the sign of the conductivity, therefore of the 6 components only three are mutually independent: σ_{xy}^{z}, σ_{zx}^{y} and σ_{yz}^{x}. In Fig. S5 we show the calculated values for the SHC and OHC in bulk MoS_2. We see clearly that SHC vanishes inside the gap, while OHC has a constant finite value. It is also evident that OHC is much higher than the values reached by SHC outside the gap, therefore the orbital current is the dominant source of angular momentum flow inside bulk MoS_2.

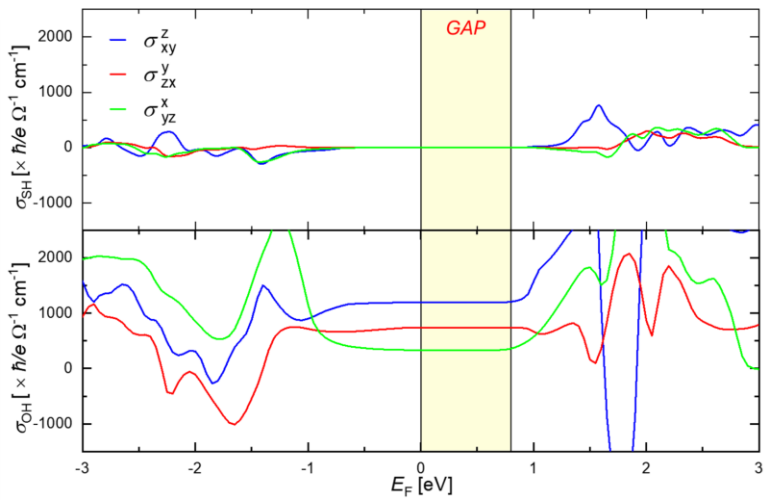

Fig. S4. Upper (lower) panel: spin (orbital) Hall conductivity of bulk MoS_2. The z-direction is parallel to the c-axis of the hexagonal structure. The x and y-direction are in-plane directions.